SIMULATION OF SEMICONDUCTOR DEVICES AND PROCESSES Vol. 3
Edited by G. Baccarani, M. Rudan - Bologna (Italy) September 26-28, 1988 - Tecnoprint

ELECTRICAL 2D SIMULATION OF 1.3 μm SEMICONDUCTOR LASER

S. Mottet and J.E. Viallet

Centre National d'Etudes des Télécommunications
BP40 - 22301 LANNION - FRANCE

SUMMARY

In this contribution, the electrical simulation of laser diodes is presented. It takes into account the specific problems related to heterojunctions. The physical model uses Fermi-Dirac statistics and thermionic emission at the interfaces. Particular attention is paid over the recombination generation mechanisms involved in the active layer: deep center, band to band and Auger recombination processes.

INTRODUCTION

Semiconductor lasers are critical components for today fiber optics 1.3 μm telecommunications. A large variety of structures, epitaxial growth techniques have been described in order to master the complex electro-optical behaviour, sensitive to technology characteristics and long term reliability of such devices.

Electrical numerical simulation of a laser must describe the heterojunctions using Fermi-Dirac statistics and thermionic emissions. The performances of the device are directly governed by the competition between the spontaneous photonic emission due to band to band recombination and deep centers and Auger recombination processes. Owing to the interfaces between the numerous epitaxial layers, adaptive mesh refinement needs to be used to correctly describe the structure within a reasonable mesh size.

PHYSICAL MODEL

Conduction model

The general set of equations used to describe steady state conduction in semiconductors consists of Poisson equation and continuity equations:

$$\mathbf{div}(\epsilon \cdot \overrightarrow{\mathbf{grad}}\ \varphi) = q \cdot (n - p - C) \tag{1}$$

$$-\frac{1}{q} \cdot \mathbf{div}\ \overrightarrow{J_n} = -U \tag{2}$$

$$\frac{1}{q} \cdot \mathbf{div}\ \overrightarrow{J_p} = -U \tag{3}$$

where C is the net fixed charge density. U is the recombination generation term due to deep centers, Auger or band to band capture emission processes.

The currents in the homogeneous materials are described by the drift diffusion model:

$$\overrightarrow{J_n} = -q \cdot n \cdot \mu_n \cdot \overrightarrow{\mathbf{grad}}\ \varphi_n \ ; \ \overrightarrow{J_p} = -q \cdot n \cdot \mu_p \cdot \overrightarrow{\mathbf{grad}}\ \varphi_p \tag{4}$$

where φ_n and φ_p are the electron and hole electrochemical potentials used in the Fermi-Dirac distribution function. In lasers the Maxwell-Boltzmann statistics are unsuitable to describe carrier densities because of the very high level of carriers injection. So the carrier densities are described by the Fermi-Dirac statistics in the parabolic band assumption:

$$n = N_C \cdot \mathcal{F}_{1/2}\left(\frac{q \cdot \varphi + \chi - q \cdot \varphi_n}{k \cdot T}\right) \ ; \ p = N_V \cdot \mathcal{F}_{1/2}\left(\frac{-q \cdot \varphi - \chi - E_g + q \cdot \varphi_p}{k \cdot T}\right) \tag{5}$$

where χ is the electron affinity and E_g the band gap energy of the local semiconductor. The $\mathcal{F}_{1/2}$ Fermi integral can be described with appropriate approximations. Viallet (1985) showed how this set of equations can be solved with respect to φ, φ_n, φ_p as main unknowns.

At abrupt heterojunction interfaces, the possible conduction mechanisms are thermionic emission and tunnel effect. For low doped semiconductors, the thermionic emission

governs the conduction at room temperature. Let us consider two semiconductor a and b such as $\chi_a > \chi_b$. The electron thermionic emission current at the interface is

$$(6) \qquad J_n = -q \cdot v_{nb} \cdot n_b \cdot \left[1 - exp\left(\frac{q \cdot \varphi_{nb} - q \cdot \varphi_{na}}{k \cdot T}\right)\right]$$

If $\chi_a + E_{ga} < \chi_b + E_{gb}$ the hole thermionic current is

$$(7) \qquad J_p = q \cdot v_{pb} \cdot p_b \cdot \left[1 - exp\left(\frac{q \cdot \varphi_{pb} + q \cdot \varphi_{pa}}{k \cdot T}\right)\right]$$

with n_b and p_b described by (5).

For a Maxwellian distribution on the b side of the interface, the thermal velocities are given by (Crowell and Sze, 1966)

$$(8) \qquad v_n = \sqrt{\frac{k \cdot T}{2 \cdot m_n^* \cdot \pi}} = \frac{A_n^* \cdot T^2}{q \cdot N_C} \quad ; \quad v_p = \sqrt{\frac{k \cdot T}{2 \cdot m_p^* \cdot \pi}} = \frac{A_p^* \cdot T^2}{q \cdot N_V}$$

where $m_{n,p}^*$ is the effective mass and $A_{n,p}^*$ the effective Richardson constant for electrons, holes.

As previously discussed by Mottet and Viallet (1988), the effective barrier heights of band discontinuities depend on the interface thickness taken into account in numerical simulation.

The tunnel emission occurs in heavily doped semiconductors which induce very high electric field regions at the interface. This effect which allows the carriers to directly cross thin barriers, can be appoximated as the barrier lowering at the interface. In the present case, this effect is not effectively described, but roughly taken into account by ensuring the barrier height lowering by controlling the interface thickness.

Generation-recombination models

The total generation-recombination term U takes into account the three main phenomena involved up to the threshold current: the deep center thermal carrier recombination U_T, the

spontaneous interband photon emission U_{sp}, the Auger recombination U_A. Since Fermi-Dirac statistics are used to describe carrier concentrations, all these recombination terms must also be described within the same statistics as proposed by Viallet and Mottet (1985).

- Deep center recombination:

This term describes the carriers generation-recombination due to carrier emissions and captures on centers with energy levels in the band gap of the semiconductor. For a center of energy E_T, the expression used is similar to the commonly used Shockley Read Hall term established for Maxwell-Boltzmann statistics, apart from the expressions of n_1 and p_1 which change for the Fermi-Dirac statistics.

$$(9)\quad U_T = \frac{n \cdot p - n_1 \cdot p_1}{\tau_n \cdot (p + p_1) + \tau_p \cdot (n + n_1)} \quad with \quad \begin{cases} n_1 = n \cdot exp\left[\dfrac{E_T + q \cdot \varphi_n}{k \cdot T}\right] \\ p_1 = p \cdot exp\left[\dfrac{- E_T - q \cdot \varphi_p}{k \cdot T}\right] \end{cases}$$

Summation over all the centers should be performed. In fact the knowledge of the whole deep center spectrum of each layer of the device is not available. It is assumed that the whole thermal recombination can be described by considering, in each layer, one dominant deep level center with energy level E_T and carriers extrinsic lifetimes τ_n, τ_p. This main recombination term which is responsible for the current of conventional non radiative diodes cannot be neglected in electroluminescent and laser diodes. Numerical or analytical models of the device current often suppose one main equivalent deep center at the middle of the gap to describe all the thermal recombination transitions. We suppose that one of the deep centers can be predominant, but there is no reason for its energy to lie at mid gap.

Moreover, the numerical computations show that the low current voltage characteristic slope of the laser depends on the value of the energy E_T of the deep center in the gap of the active layer. The energy E_T is one of the input parameters of the numerical model as well as τ_n and τ_p.

▪ Interband spontaneous optical emission:

The interband spontaneous optical emission can be described by

$$(10)\quad U_{sp} = B_0 \cdot (n \cdot p - n_0 \cdot p_0) \text{ with } n_0 \cdot p_0 = n \cdot p \cdot exp\left[\frac{q \cdot \varphi_n - q \cdot \varphi_p}{k \cdot T}\right]$$

where $n_0 \cdot p_0$ expression involves Fermi-Dirac statistics even at thermodynamical equilibrium.

The total spontaneous radiant power of the structure is obtained by integrating U_{sp} over the volume of the active layer.

▪ Auger recombination:

When both electron and hole densities attain high values such as those obtained in the active layer of a 1.3 µm operating laser, the Auger recombination processes are dominant. Under high injection condition, $n \simeq p$ in the active layer, so that a mean value for hole and electron processes may be used to express Auger recombination.

$$(11)\quad U_A = C_A \cdot (n + p) \cdot (n \cdot p - n_0 \cdot p_0);\ n_0 \cdot p_0 = n \cdot p \cdot exp\left[\frac{q \cdot \varphi_n - q \cdot \varphi_p}{k \cdot T}\right]$$

LASER STRUCTURE

The results presently described concern 1.3 µm buried heterostructure laser. Figure 1 shows the cross section of the modeled laser. The active layer Q is $Ga_{.25}In_{.75}As_{.57}P_{.43}$ residual N type undoped compound ($C = 10^{15} cm^{-3}$). The lateral dimensions of the structure and the thickness of the N^+ InP substrate are smaller than in actual devices to reduce computationnal effort, since it does not modify the behaviour of the effective part of the device.

Most of the physical parameters, such as effective masses and forbidden bandgap energies, are those published in the litterature, as a function of temperature (Tsang, 1985). Among these laws, more attention was taken concerning the band to band spontaneous emission constant B_0 and the Auger coefficient C_A which are critical parameters for the description of the quaternary layer behaviour. The 1.3 µm spontaneous emission

in $GaInAsP$ is $B_0 = 10^{-10} \cdot (T/300)^{1.5}\ cm^3 \cdot s^{-1}$. This value has been checked by diode measurements performed at 77 K.

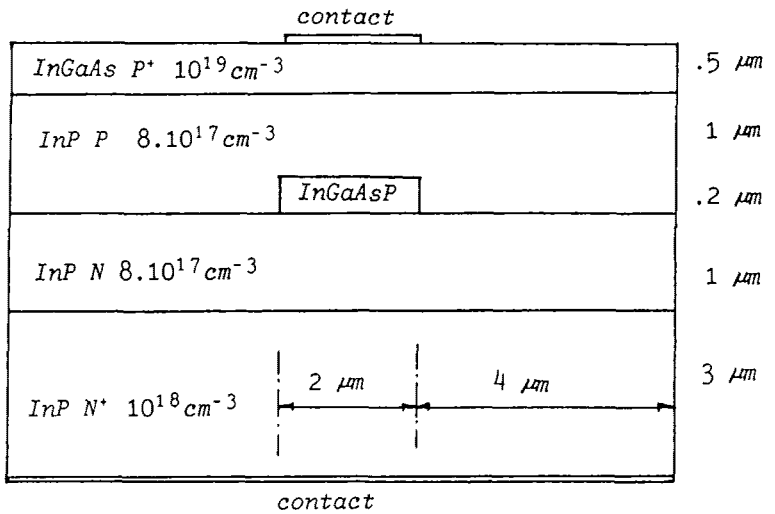

Fig. 1. Cross section of the buried heterostructure laser

At this temperature, thermal and Auger recombinations decrease and may be neglected with regard to the band to band spontaneous emission current. Some discrepancy on the Auger coefficient appears in the litterature. Among the possible values, $C_A = 3.6\ 10^{-27} \cdot exp[-1280/T]\ cm^6 \cdot s^{-1}$ in the quaternary layer has been choosen ($C_A = 5\ 10^{-29}\ cm^6 \cdot s^{-1}$ at room temperature).

NUMERICAL MODELS

The first model deals with one dimensionnal simulation of the cross section of figure 1 through the quaternary layer, since the active layer drives predominantly the current flowing into the device. Finite difference method have been used to solve the set of equations as a function of φ, φ_n, φ_p (Mottet and Viallet, 1988; Viallet and Mottet, 1985).

The band diagram of the .9 V forward biased laser is showned in figure 2. Such a bias corresponds to high carrier injection level before the lasing threshold current. Fermi-Dirac statistics must be used owing to the high carrier

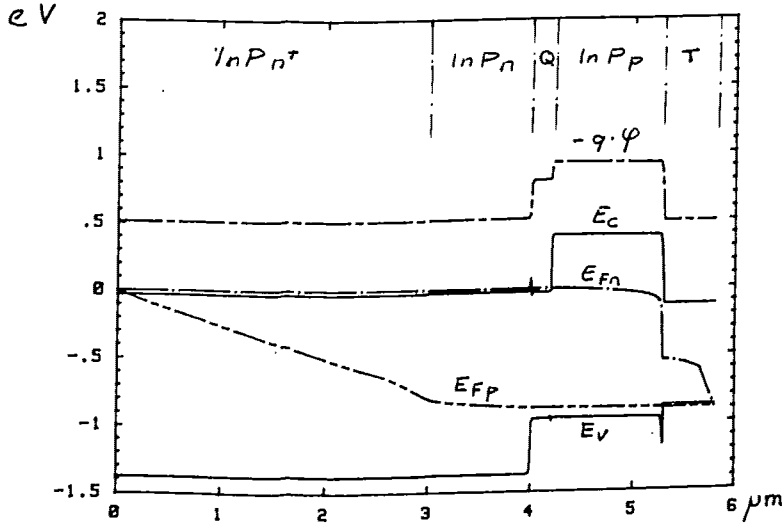

Fig. 2. Band diagram of the .9 V forward biased laser

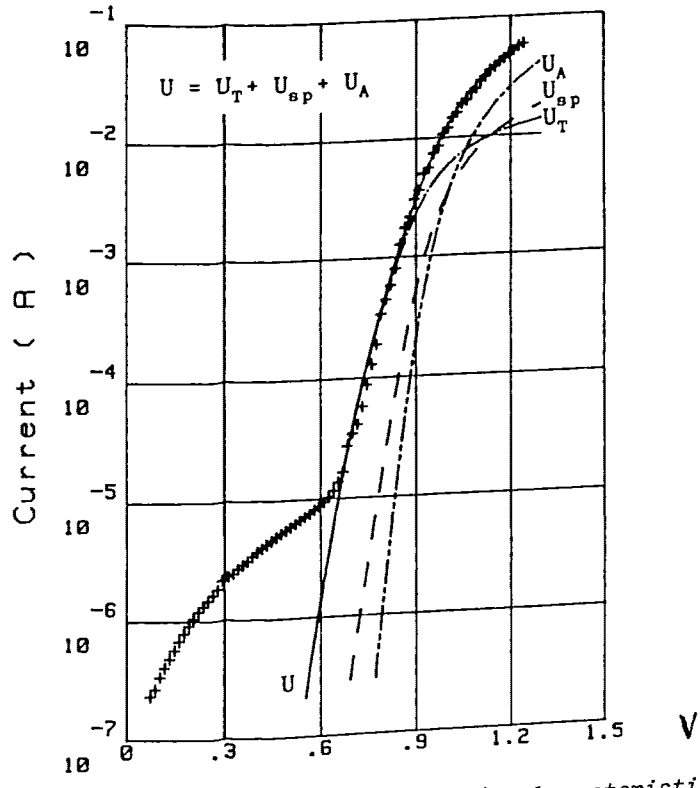

Fig. 3. Experimental and computed I(V) characteristics and contributions of the three recombination mechanisms.

densities in the quaternary. The electron Fermi level has already crossed the conduction band, although the laser is not yet under nominal bias. Therefore the forward $I(V)$ characteristic may not be described by a standard diode exponential behaviour. At the *InGaAs/InP* interface, barrier lowering must be controlled to assure hole conduction which should have been described by a tunnel effect in these highly doped materials. For an abrupt heterojunction, the thermionic emission alone would have lead to an abnormal drop of the Fermi level and to a limitation of the conduction. The computed $I(V)$ characteristic is compared to experimental measurements (Fig. 3.) of a Thomson-CSF BH laser diode performed with MOCVD epitaxial growth. This simulation result has been obtained by fitting the carrier lifetimes in the quaternary layer to $\tau_n = \tau_p = 2 \cdot 10^{-9} s$. Serial resistance effect, due to the ohmic

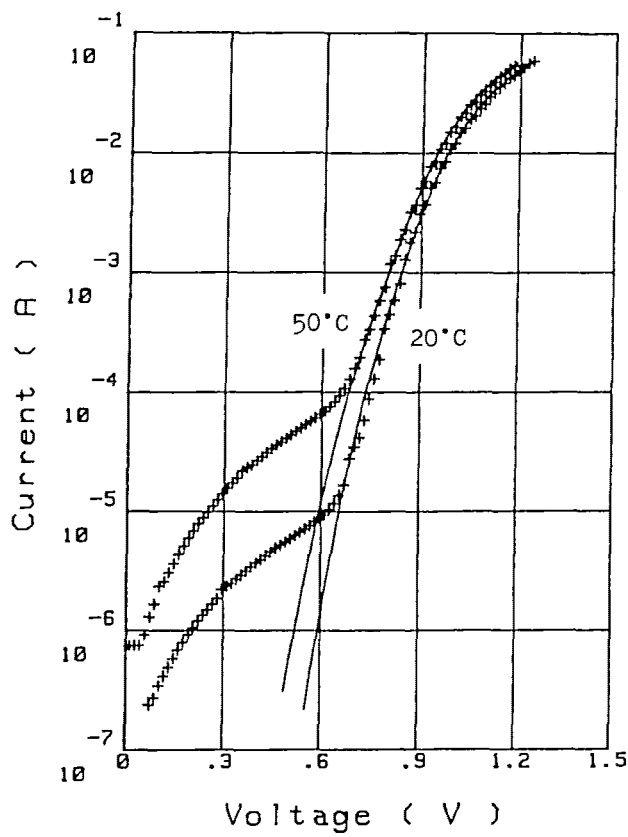

Fig. 4. Experimental and modeled characteristics at 20 and 50°C

contacts, has been added to fit the very high current range (Mottet and al, 1987). In this figure, the different recombination term contributions are plotted.

Apart from the very low current range, the temperature dependant physical model and simulation results are in very good agreement with experimental datas at different temperatures as it is showned in figure 4.

The second model is a two dimensionnal model of the structure described in figure 1. Owing to symmetry properties, only the righ handside of the structure is simulated, with adequate Neumann boundary conditions. The purpose of this simulation is to exibit the current behaviour at the corner edge of the quaternary layer, leading to a defocalization effect. In order to minimize the mesh size, an adaptive mesh method has been used. Since lasers are forward biased, the electric fields are maximum at thermodynamical equilibrium. When biased, the Fermi levels exibit smooth variations quite similar, throughout the structure, to those presented in fig. 2. Therefore, the maximum of the three potentials second derivative are obtained at thermodynamical equilibrium. For these reasons, the mesh is optimize at thermodynamical equilibrium. Over a initial regular mesh, segments are divided in two in relation with the computed refinement criteria. This criteria consists in the calculation of the error on carrier densities induces by the second order derivative of the electrostatic potential in the linearization scheme used. Only Poisson non linear equation needs to be solved. The final mesh is shown in figure 5.

The electrostatic potential map for .9 V forward bias given in figure 6. The $3D$ map representations do not respect spatial dimensions but correspond to the value of the function on the nodes matrix, thus allowing to detail areas of large variations. This figure demonstrates the $2D$ electric field effect at the edges of the quaternary layer.

The total current direction and intensity is very sensitive to the two dimensionnal behaviour of the structure. Figures 7.a and 7.b are the projections of the total density current vector, $\overrightarrow{J_T} = \overrightarrow{J_n} + \overrightarrow{J_p}$, over the x and y directions. For the x projection (fig. 7.a) the negative value in the InP N material corresponds to the focalization of the current flow into the quaternary layer which was predictible. Less

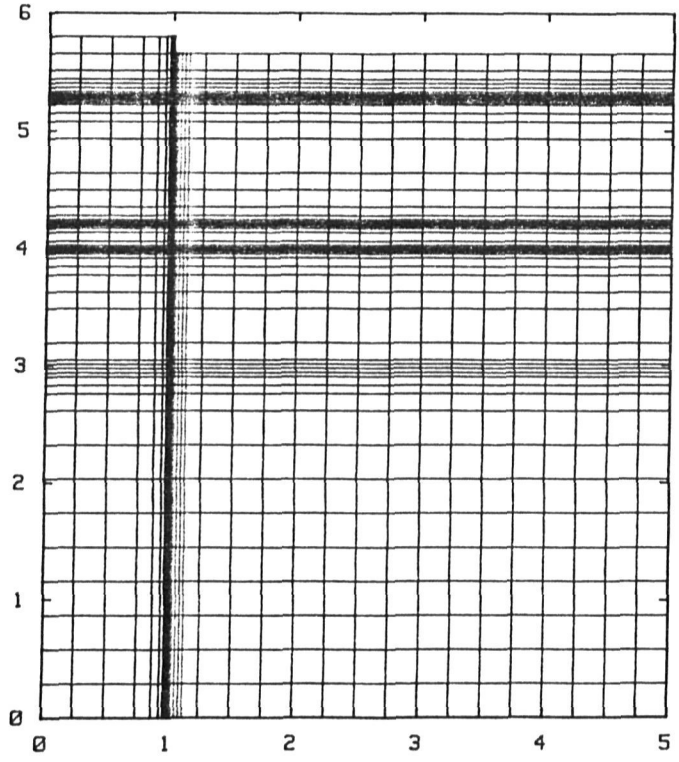

Fig. 5. Laser structure mesh.

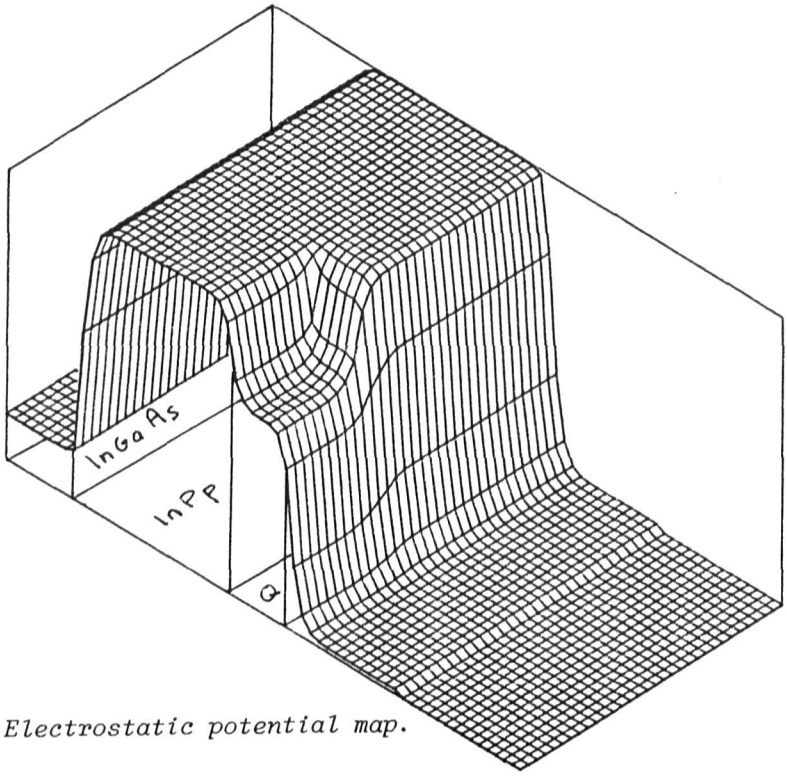

Fig. 6. Electrostatic potential map.

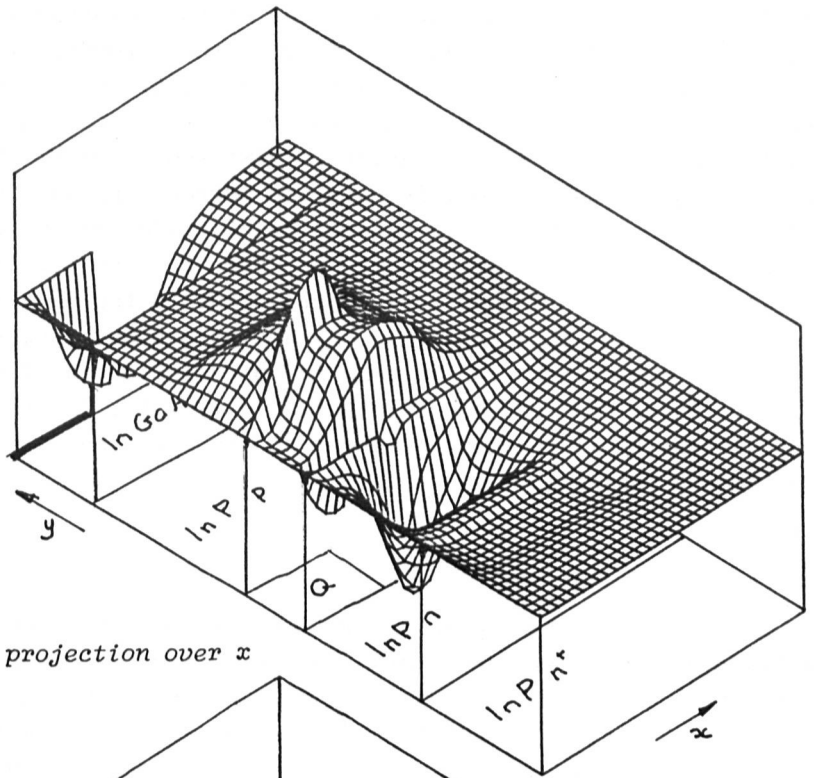

a) projection over x

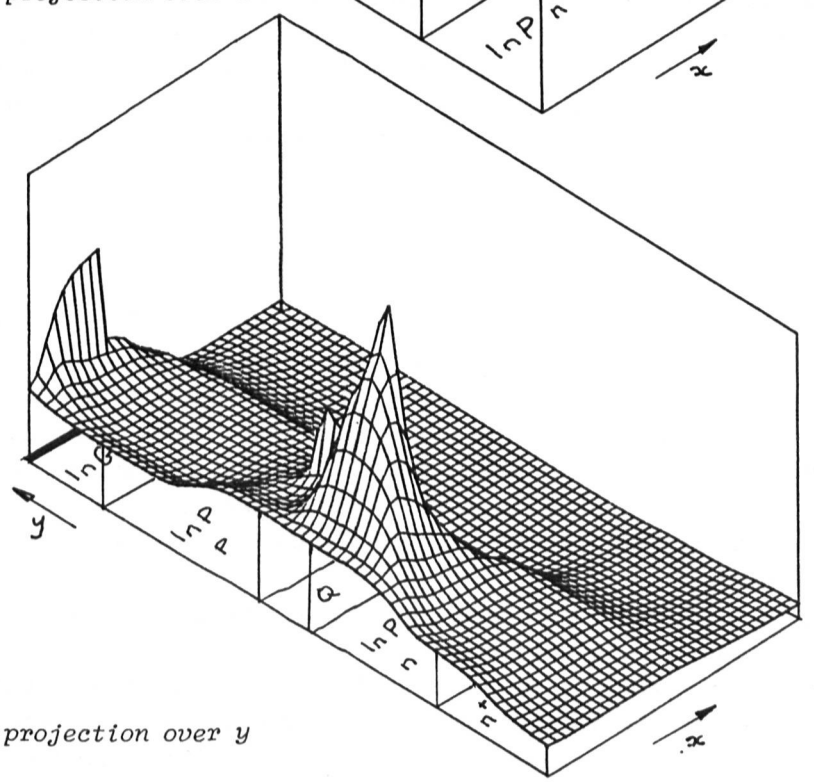

b) projection over y

Fig. 7. Map projections of the total current.

predictible are the lateral current flows at the interfaces of the quaternary layer. The negative flow at the interface with *InP N* corresponds to the normal current focalization, but the positive flow at the *InP P* interface indicates a defocalization of the current although the *P* contact is just above and has the width of the quaternary layer. In fact the current spreads into the resistive *P InP* material, before being collected by the *P InGaAs* layer, which drives it at the *P* contact. The collection effect of *InGaAs* layer corresponds to the negative current flowing in this material. As a consequence, larger y projection of the current can be seen at the right edges of the quaternary layer and of the *P* contact (fig. 7.b). The total current intensity is very much larger at the edge than inside the quaternary, which may lead to hot points.

CONCLUSION

In this paper, physical models of the conduction mechanisms and generation-recombination processes involved in 1.3 μm laser diode are discussed. The numerical simulations performed, using this temperature dependant model, allow to obtain the electrical characteristic of the laser and provide for a valuable understanding of the two dimensionnal behaviour of the structure.

REFERENCES

Crowell C.R. and Sze S.M. (1966), Current transport in metal semiconductors barriers, *Solid State Electron.*, *9*, 1035.

Mottet S. and al. (1987), Analysis and modelling of 1.3 μm laser diodes, *Proceeding of Int. Symp. GaAs and Related Compounds*, Inst. Phys. Conf. Ser. No 91:chap. 7, pp. 621-624

Mottet S. and Viallet J.E. (1988), Thermionic emission in heterojunctions, *Proceeding of SISDEP III Conf*, to be published.

Tsang W.T. (1985), *Semiconductors and Semimetals*, Vol 22, part C, Academic Press, Orlando.

Viallet J.E. and Mottet S. (1985), Heterojunctions under Fermi-Dirac statistics:general set of equations and steady state numerical methods, in J.J.H. Miller (Ed.), *Proceeding of NASECODE IV Conf.*, Boole Press, Dublin, pp. 530-535.